Electronic Supplementary Material (ESI) for ChemComm.

Supplementary Information: Correlating Blocking Temperatures with Relaxation Mechanisms in Single-Molecule Magnets

Marcus J. Giansiracusa, Andreas K. Kostopoulos, David Collison, Richard E. P. Winpenny* and Nicholas F. Chilton*

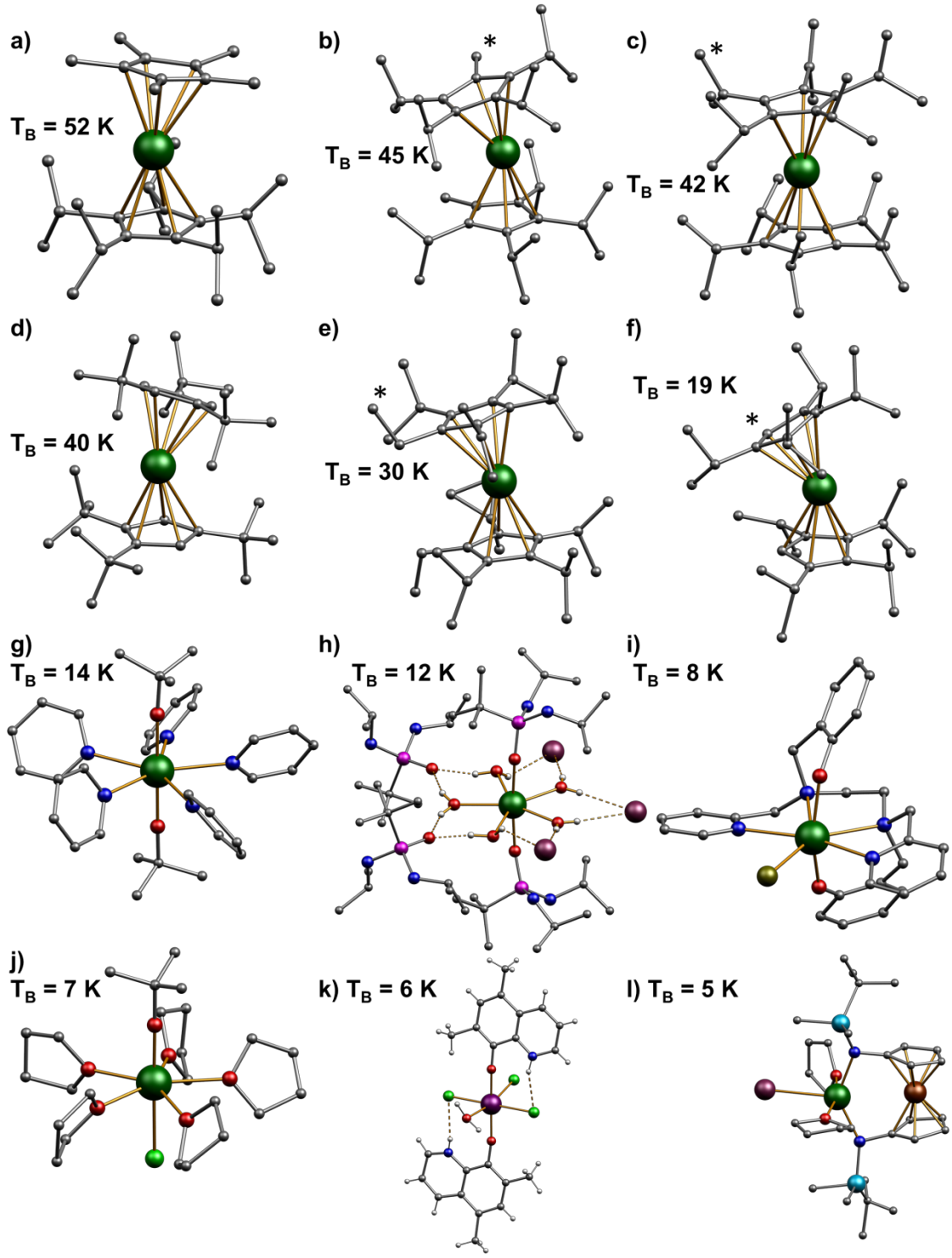

Figure S1. Molecular structure of high barrier SMM systems included in literature investigation, (**a**) $[Dy(Cp^*)(Cp(^iPr)_5)]^+$ (**b**) $[Dy\{Cp(^iPr)_4(Me)\}_2]^+$, (**c**) $[Dy\{Cp(^iPr)_5\}_2]^+$, (**d**) $[Dy(Cp^{ttt})_2]^+$, (**e**) $[Dy\{Cp(^iPr)_4(Et)\}_2]^+$, (**f**) $[Dy\{Cp(^iPr)_4\}_2]^+$, (**g**) $[Dy(O^tBu)_2(py)_5]^+$, (**h**) $[^tBuPO(NH^iPr)_2Dy(H_2O)_5]^{3+}$, (**i**) [Dy(bbpen)Br], (**j**) $[Dy(O^tBu)Cl(THF)_5]^+$, (**k**) $[Dy(DiMeQ)_2Cl_3(H_2O)]$ and (**l**) $[(NN^{TBS})DyI(THF)_2]$. Counter ions and hydrogen atoms omitted for clarity. For Cp variants, the asterisk highlights the unique R group. See below for counter ions.

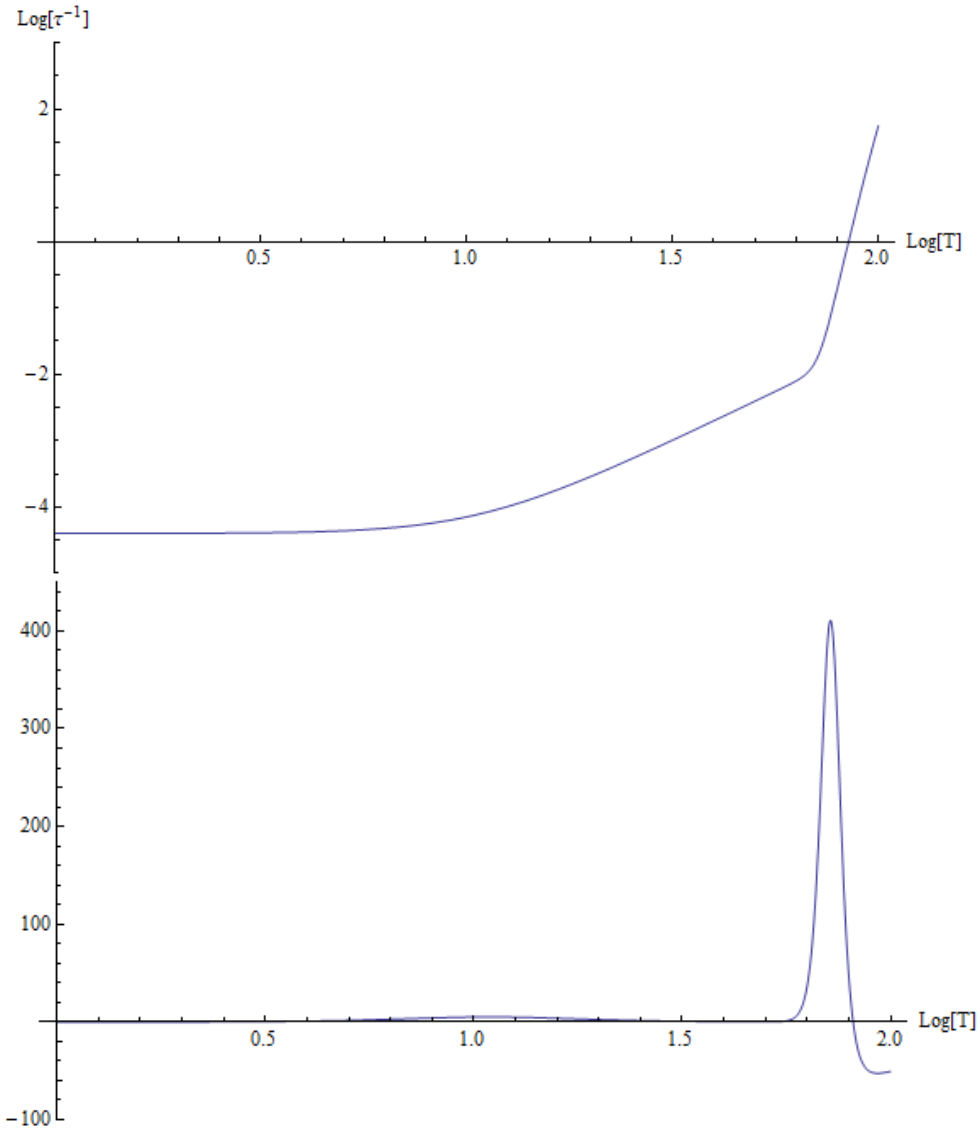

Figure S2. Relaxation rate data (**top**) for [Dy(Cp*)(Cp(^{i}Pr)$_5$)][B(C_6F_5)$_4$] plotted as log[τ^{-1}] vs log[T] using literature fitted parameters. The double derivative is illustrated **below** to indicate the determination of τ_{Switch}.

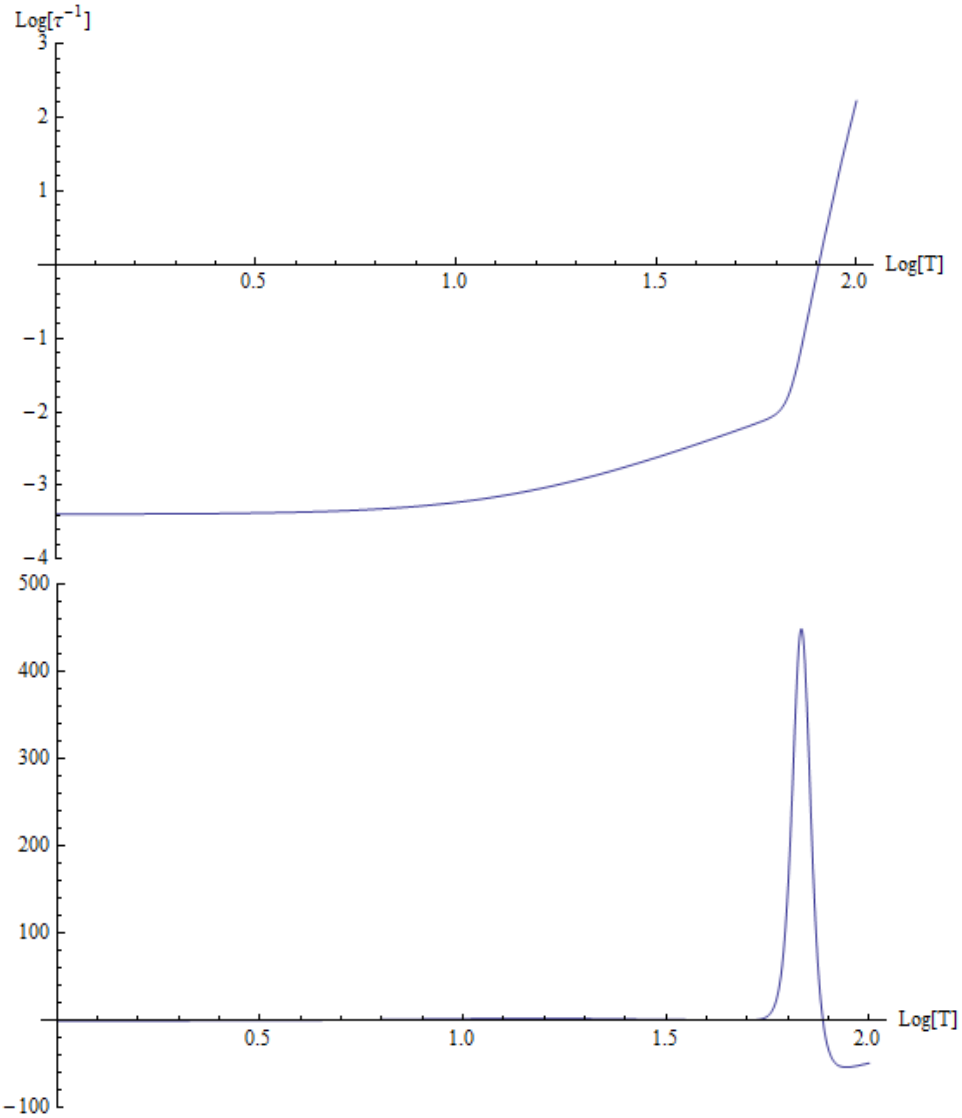

Figure S3. Relaxation rate data (**top**) for [Dy{Cp(^{i}Pr)$_4$(Me)}$_2$][B(C$_6$F$_5$)$_4$] plotted as log[τ^{-1}] vs log[T] using literature fitted parameters. The double derivative is illustrated **below** to indicate the determination of τ_{Switch}.

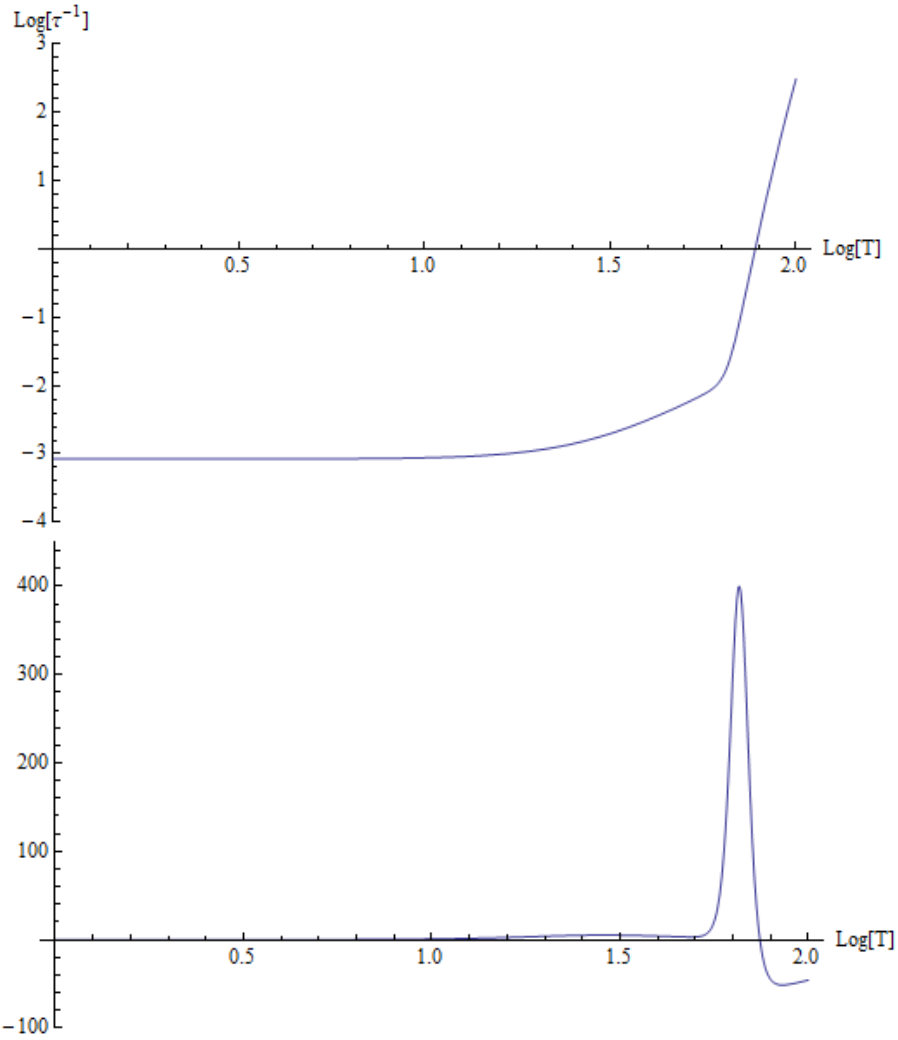

Figure S4. Relaxation rate data (**top**) for [Dy{Cp(^{i}Pr)$_4$(Et)}$_2$][B(C$_6$F$_5$)$_4$] plotted as log[τ^{-1}] vs log[T] using literature fitted parameters. The double derivative is illustrated **below** to indicate the determination of τ_{Switch}.

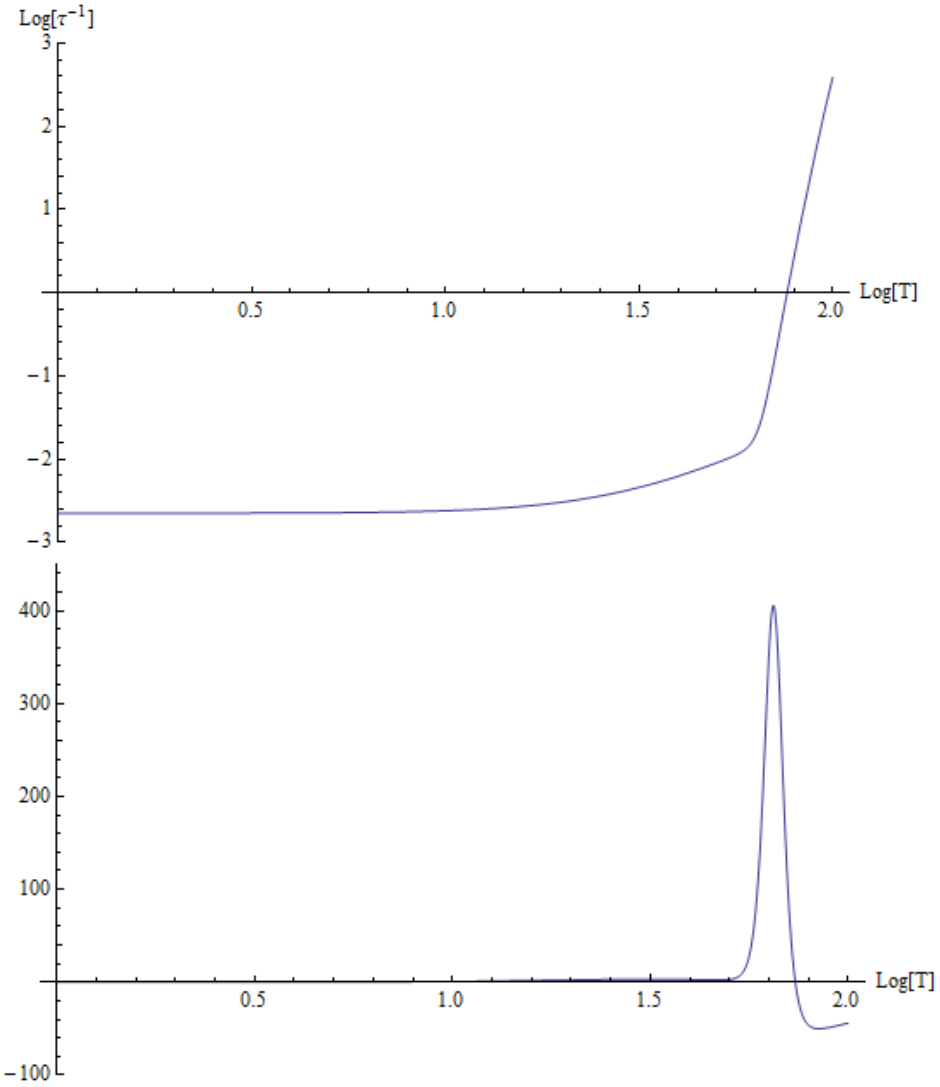

Figure S5. Relaxation rate data (**top**) for [Dy{Cp(^{i}Pr)$_5$}$_2$][B(C$_6$F$_5$)$_4$] plotted as log[τ^{-1}] vs log[T] using literature fitted parameters. The double derivative is illustrated **below** to indicate the determination of τ_{Switch}.

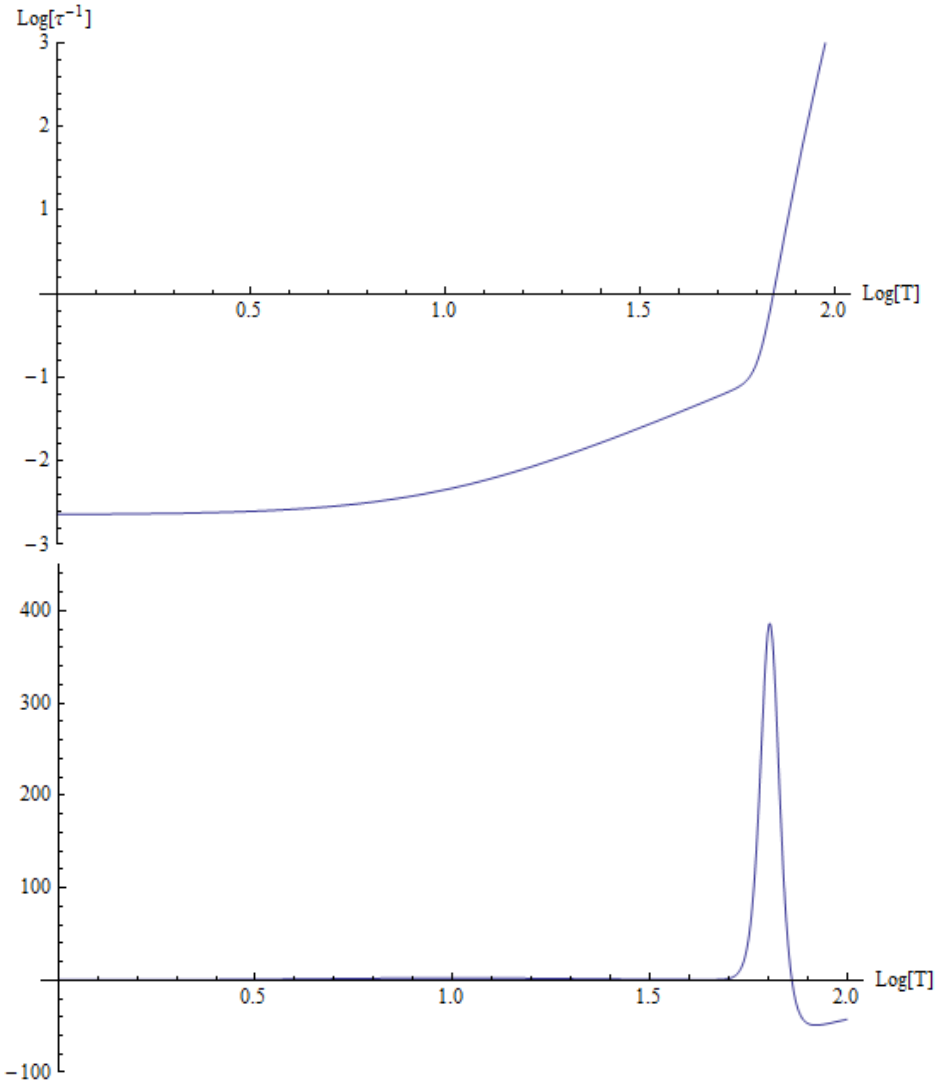

Figure S6. Relaxation rate data (**top**) for [Dy{Cp(^{i}Pr)$_4$}$_2$][B(C$_6$F$_5$)$_4$] plotted as log[τ^{-1}] vs log[T] using literature fitted parameters. The double derivative is illustrated **below** to indicate the determination of τ_{Switch}.

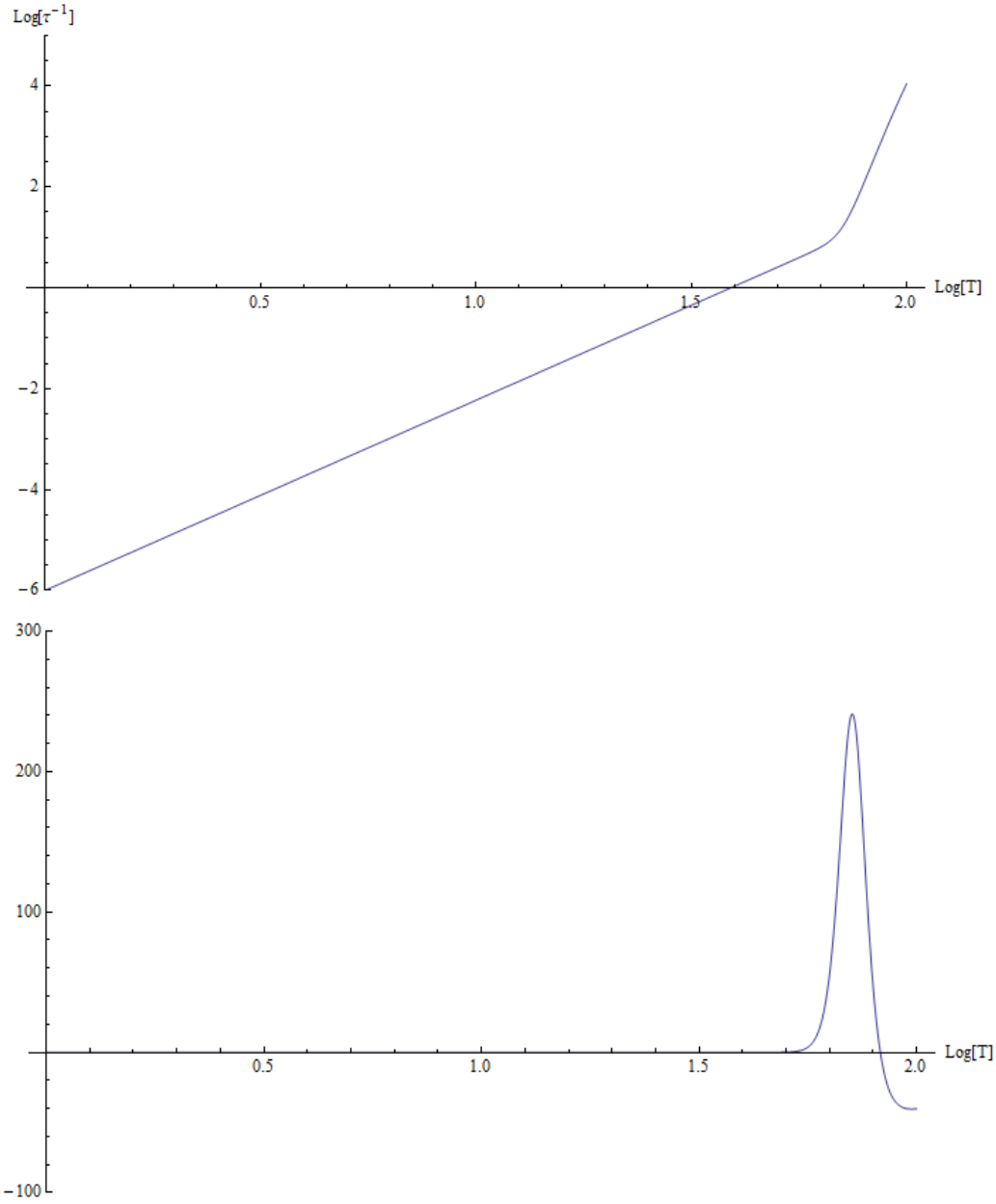

Figure S7. Relaxation rate data (**top**) for $[Dy(O^tBu)_2(py)_5][BPh_4]$ plotted as $\log[\tau^{-1}]$ vs log[T] using literature fitted parameters. The double derivative is illustrated **below** to indicate the determination of τ_{Switch}.

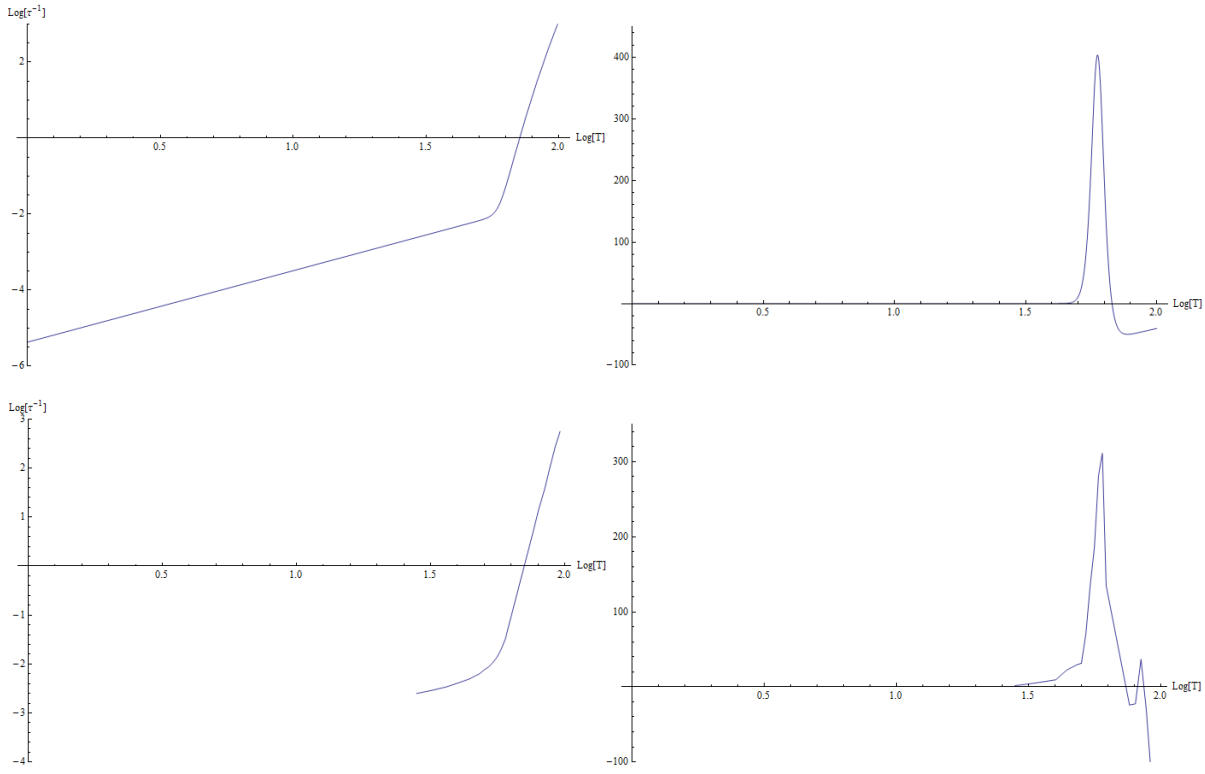

Figure S8. Relaxation rate data (**left**) for $[Dy(Cp^{ttt})_2][B(C_6F_5)_4]$ plotted as $\log[\tau^{-1}]$ vs log[T] using literature fitted parameters (**top**) and literature experimental data (**bottom**). The double derivatives are illustrated **right** to indicate the determination of τ_{Switch} for bot fitted data (**top**) and experimental data (**bottom**). The numerical approach yields a similar τ_{Switch} value of 52.01 s.

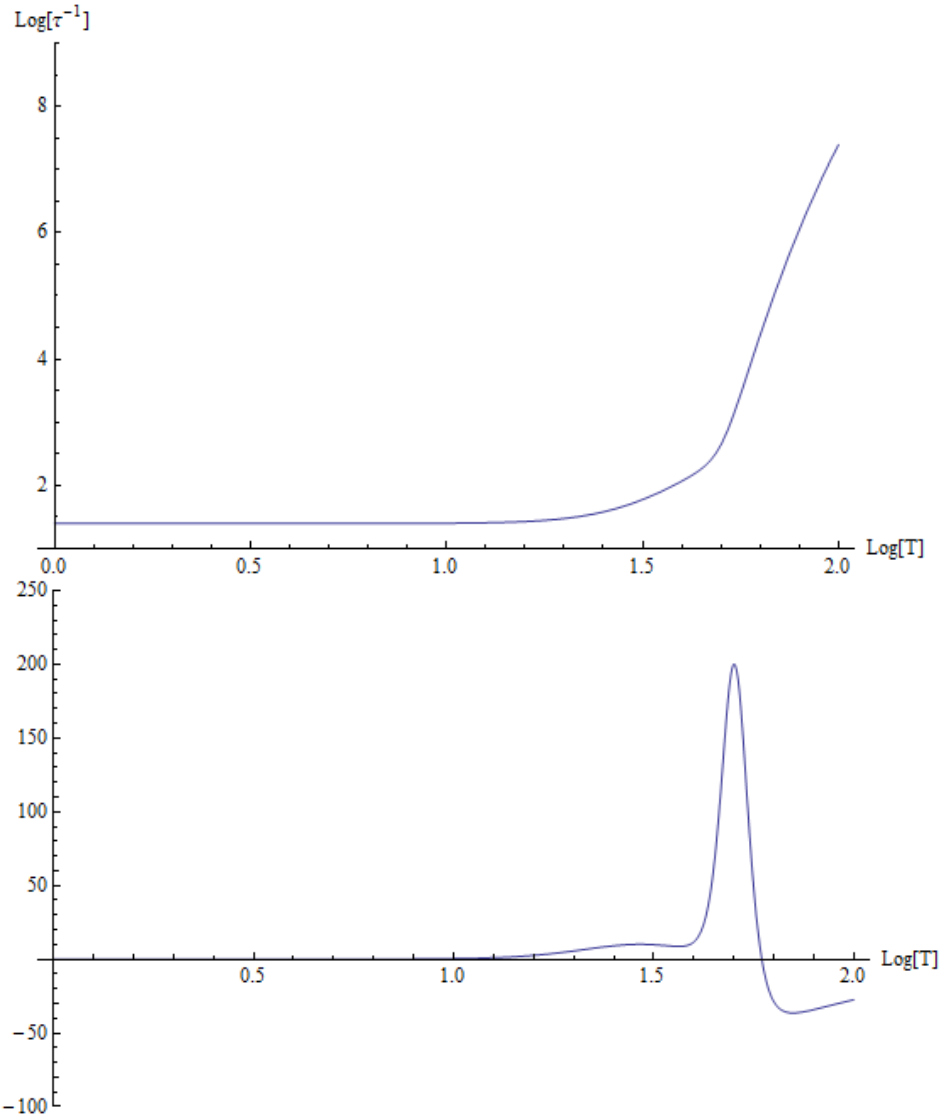

Figure S9. Relaxation rate data (**top**) for [Dy(bbpen)Br] plotted as log[τ^{-1}] vs log[T] using literature fitted parameters. The double derivative is illustrated **below** to indicate the determination of τ_{Switch}.

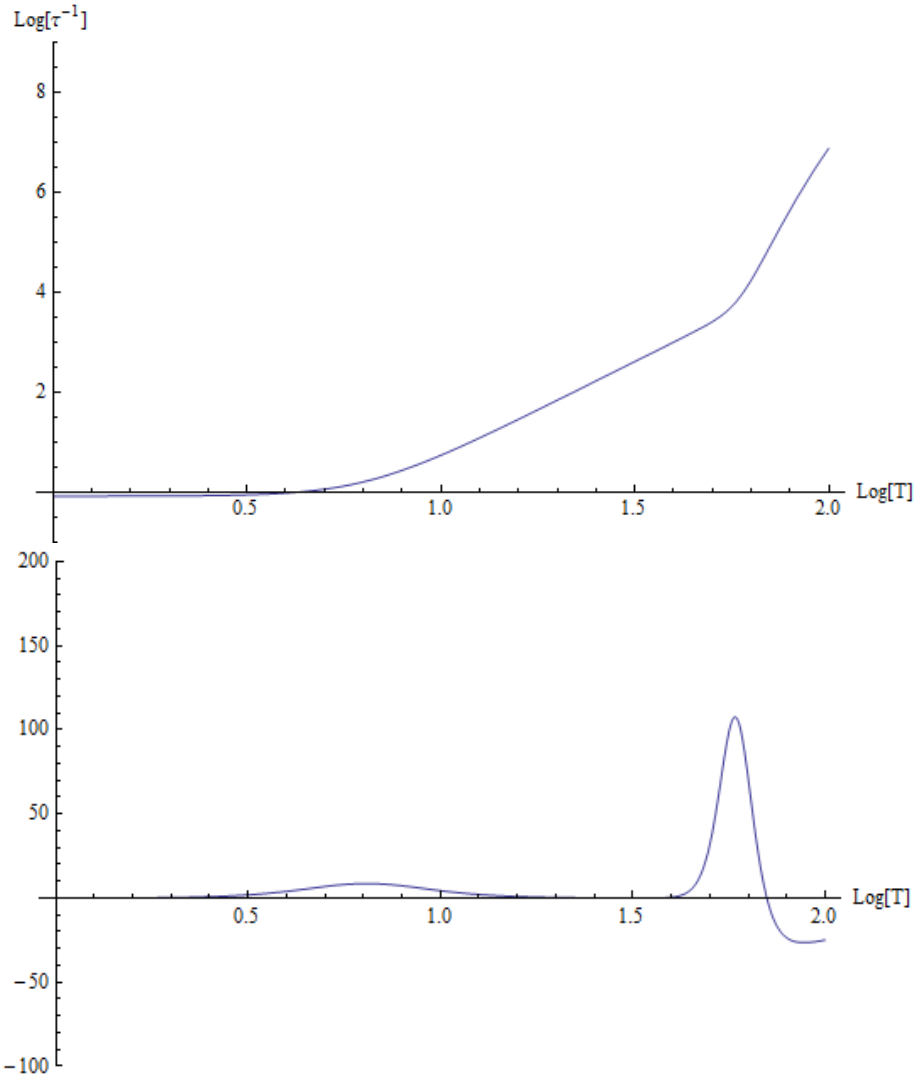

Figure S10. Relaxation rate data (**top**) for $[Dy(DiMeQ)_2Cl_3(H_2O)]$ plotted as $\log[\tau^{-1}]$ vs log[T] using literature fitted parameters. The double derivative is illustrated **below** to indicate the determination of τ_{Switch}.

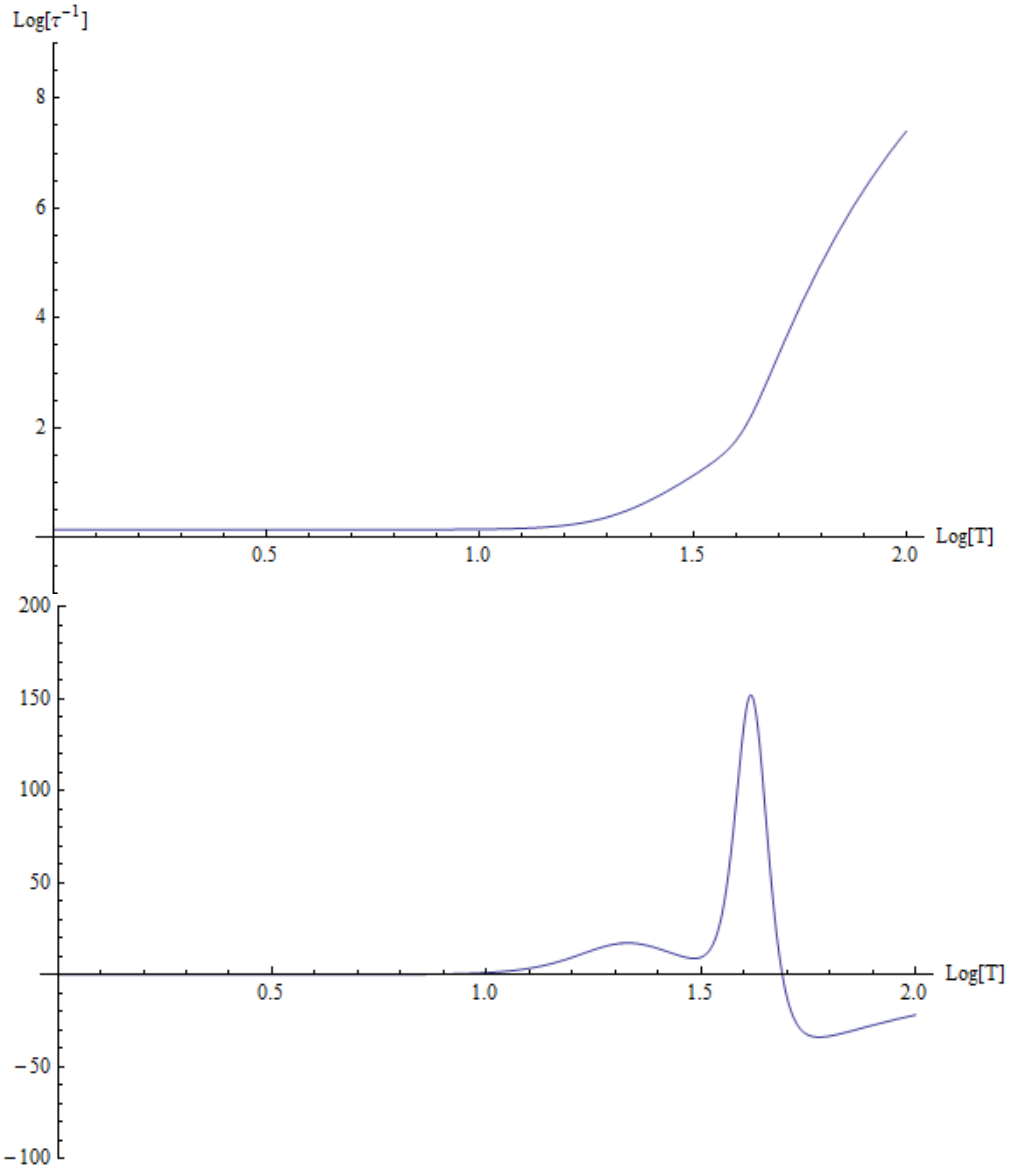

Figure S11. Relaxation rate data (**top**) for [Dy(O^{t}Bu)Cl(THF)][BPh$_4$] plotted as log[τ^{-1}] vs log[T] using literature fitted parameters. The double derivative is illustrated **below** to indicate the determination of τ_{Switch}.

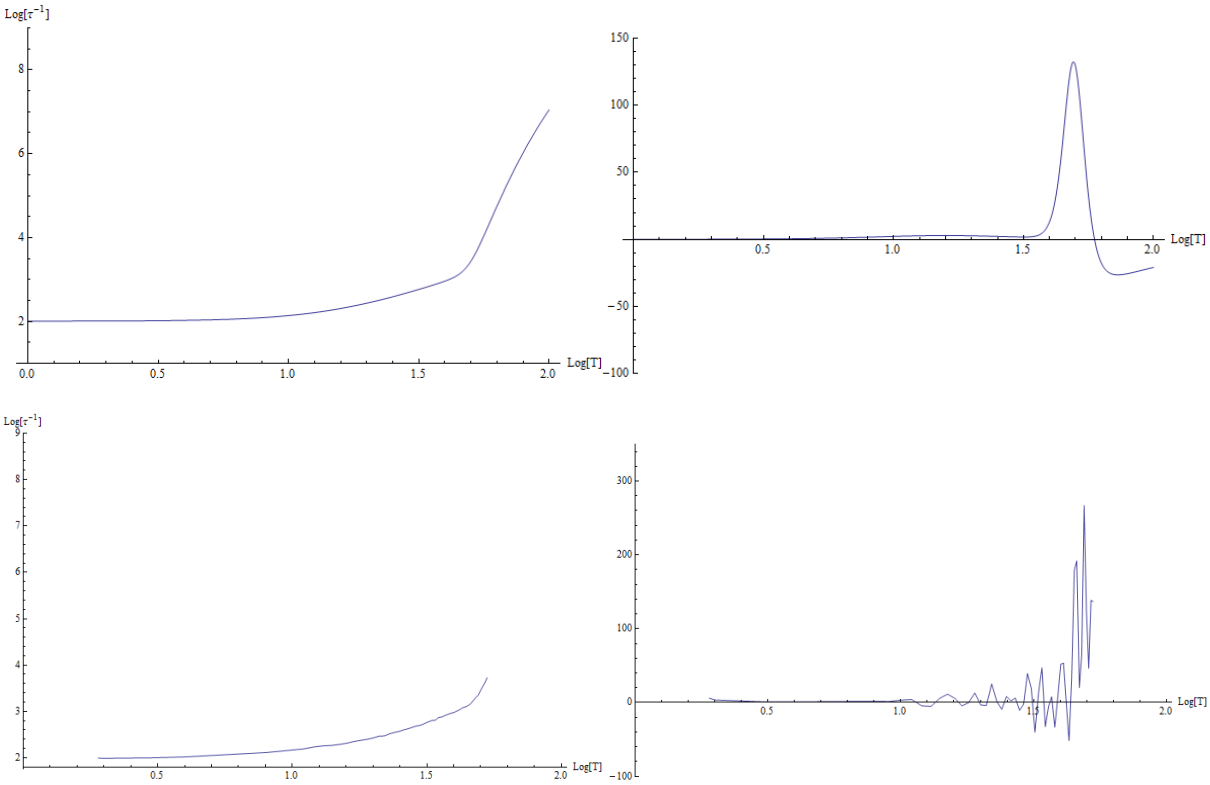

Figure S12. Relaxation rate data (**left**) for [(NN^{TBS})DyI(THF)$_2$] plotted as log[τ^{-1}] vs log[T] using literature fitted parameters (**top**) and literature experimental data (**bottom**). The double derivatives are illustrated **right** to indicate the determination of τ_{Switch} for bot fitted data (**top**) and experimental data (**bottom**). The numerical approach yields a similar τ_{Switch} value of 4.45 x 10^{-4} s.

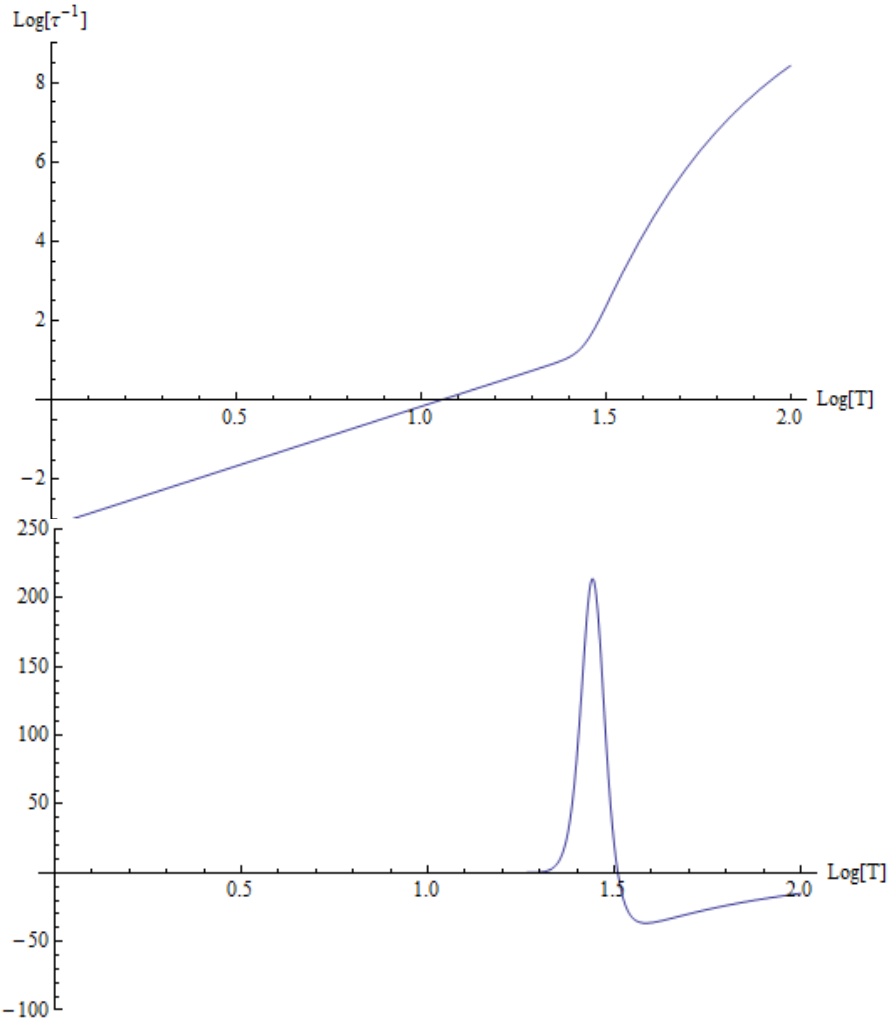

Figure S13. Relaxation rate data (**top**) for [^{t}BuPO(NH^{i}Pr)$_2$Dy(H$_2$O)$_5$][I$_3$] plotted as log[τ^{-1}] vs log[T] using literature fitted parameters. The double derivative is illustrated **below** to indicate the determination of τ_{Switch}.

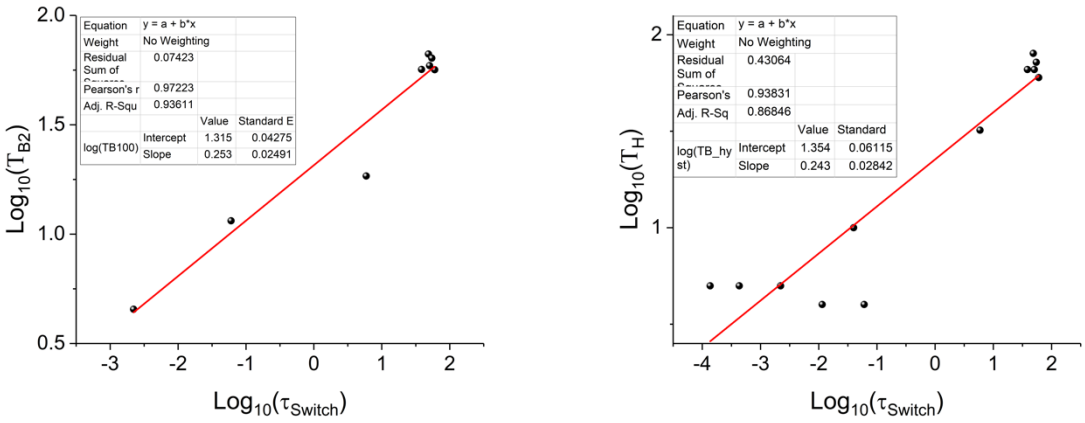

Figure S14. Log(τ_{swtich}) vs Log(T_B) using 100 s defintion of blocking temperature (T_{B2}, left) and open hysteresis temperature (T_H, right).

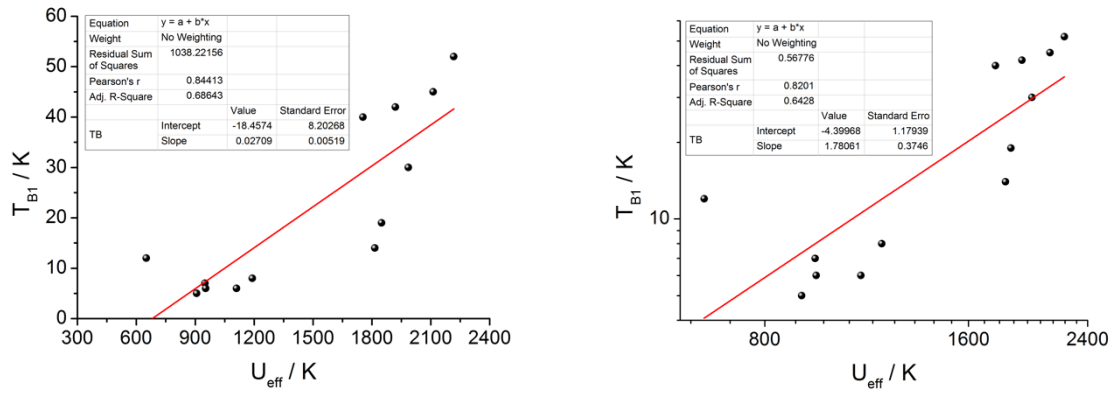

Figure S15. Left) Plot of reported U_{eff} values versus T_{B1} for the high barrier systems discussed in the main text. **Right**) Shows the same data on a log-log scale. A linear fitting of both data have been attempted giving the highest R^2 value of 0.69, far poorer correlation than for a plot of T_{B1} *versus* τ_{Switch}.

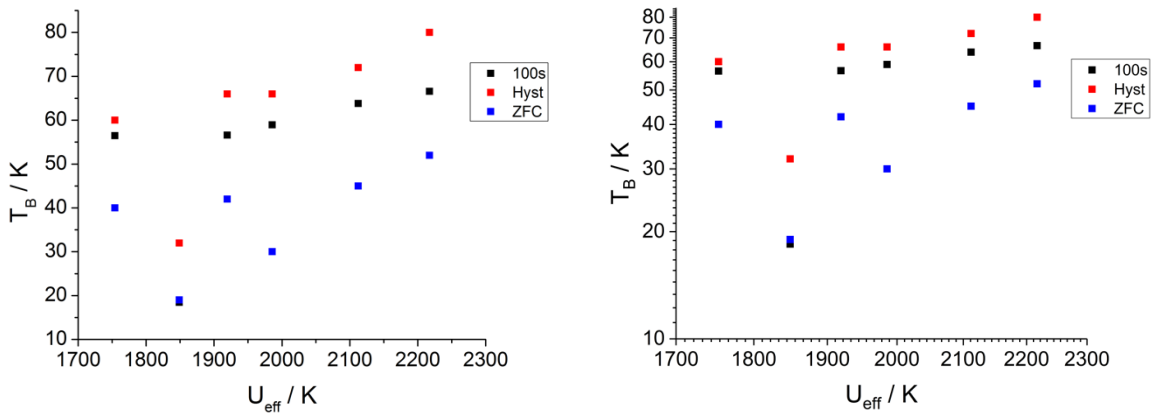

Figure S16. Plot of U_{eff} vs T_{B1} with linear (**left**) and log-scale (**right**) using each definition for the Cp variants. The definition of U_{eff} alone is unable to justify the poor performance observed for $[Dy\{Cp(^{i}Pr)_4\}_2][B(C_6F_5)_4]$ (U_{eff} = 1848).

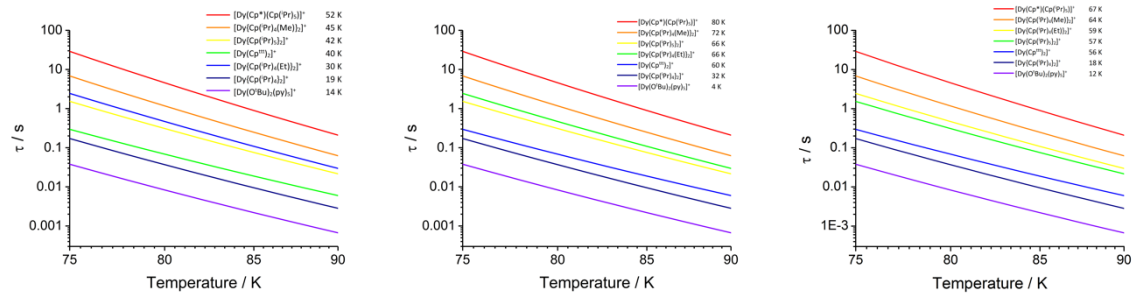

Figure S17. Plot of Orbach regime for fitted parameters of high barrier systems between 75 and 90 K, where the Obrach regime is dominant for these systems. **Left**) using ZFC peak definition for T_{B1}, **centre**) using hysteresis definition for T_H and **right**) using 100-s blocking T_{B2}.

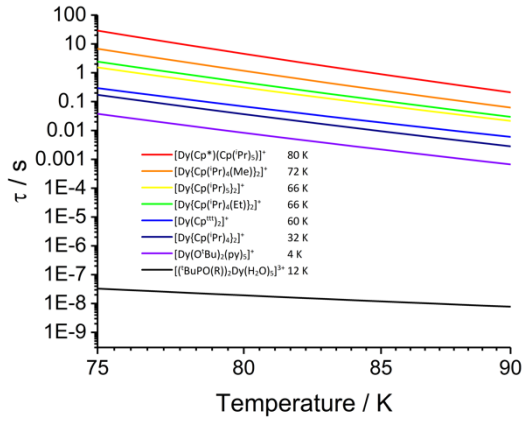

Figure S18. Plot of Orbach regime for fitted parameters of high barrier systems between 75 and 90 K including [^{t}BuPO(NH^{i}Pr)$_2$Dy(H$_2$O)$_5$][I$_3$] to highlight that this comparison cannot be extended to lower barrier systems. Despite the observation of open hysteresis up to 12 K, this system cannot be compared using Orbach because it requires extrapolation beyond the temperature at which slow relaxation is observed.

Table S1. Collection of Er based SMMs from literature. COT = cyclooctatetraenide, Dsp = 3,4-dimethyl-2,5-bis(trimethylsilyl)phospholyl, COT" = 1,4-bis(trimethylsilyl)cyclooctatetraenyl and Cp* = pentamethylcyclopenta-dienyl.

Er SMMs	U_{EFF} (k)	T_0 (s)	T_B Hyst (K)	REF
[Er(COT)(Dsp)]	358	1.60 x 10^{-11}	10	S1
[K(18-crown-6)][Er(COT)$_2$]	216	6.90 x 10^{-8}	10	S2
[Er(COT)Cp*]	323	8.17 x 10^{-11}	5	S3
	197	3.13 x 10^{-9}		S3
[K(18-crown-6)][Er(COT)$_2$]	286	3.70 x 10^{-9}	5	S4
[Er(COT)(C$_5$H$_5$B)]	373	5.30 x 10^{-12}	8	S5
[Er(COT)(C$_5$H$_5$BMe)]	432	5.50 x 10^{-12}	6	S5
[Er(COT)(C$_5$H$_5$BNEt$_2$)]	250	9.20 x 10^{-10}	2	S5
[Li(DME)$_3$][Er(COT'')$_2$]	187	4.00 x 10^{-8}	8	S6
[Er$_2$(COT")$_3$]	323	5.70 x 10^{-10}	7	S7
[K$_2$(THF)$_4$][Er$_2$(COT")$_3$]	306	5.00 x 10^{-9}	10	S7
[Er{N(SiMe$_3$)$_2$}$_3$]	122	9.33 x 10^{-9}	-	S8

Table S2. Collection of Tb based SMMs from literature, all systems show no open hysteresis above 2 K. Pc = phthalocyaninato, TPP = tetraphenylporphyrin, DBU = 1,8-diazabicyclo[5.4.0] undec-7-ene and Cp* = pentamethylcyclopenta-dienyl.

Tb SMMs	U_{eff} **(K)**	T_0 **(s)**	**REF**
$[Tb(Pc)_2]$	590	1.5×10^{-9}	S9
$[Tb\{(OEt)_8Pc\}_2]$	791	4.2×10^{-11}	S10
$[Tb(Pc)(PcR_8)]$ R = $O(C_6H_4)$-*p*-^{t}Bu	725	2.2×10^{-11}	S11
$[Tb(Pc)(PcR_8)]$ R = $O(C_6H_4)$-*p*-^{t}Bu	938	1.1×10^{-11}	S11
$[Tb(Pc)(Pc(R1)_4(R2)_4]$ R1 = ^{t}Bu R2 = H	924	2.2×10^{-11}	S11
$[NMe_4][Tb(PcR_8)_2]$ R = $O(C_6H_4)$-*p*-^{t}Bu	636	8.3×10^{-11}	S11
$[NBu_4][Tb(PcR_8)_2]$ R = $O(C_6H_4)$-*p*-^{t}Bu	567	3.4×10^{-10}	S11
$[NMe_4][Tb(Pc)(PcR_8)]$ R = $O(C_6H_4)$-*p*-^{t}Bu	648	3.0×10^{-10}	S11
$[NBu_4][Tb(Pc)(PcR_8)]$ R = $O(C_6H_4)$-*p*-^{t}Bu	701	7.7×10^{-11}	S11
$[NBu_4][Tb(Pc)(Pc(R1)_4(R2)_4]$ R1 = ^{t}Bu R2 = H	576	4.8×10^{-10}	S11
$[HDBU][Tb(TPP)_2]$	387	1.6×10^{-11}	S12
$[Tb(Cp^*)_2(BPh_4)]$ (dilute)	344	1.0×10^{-10}	S13
		$\tau_{Switch} = 3.8 \times 10^{-4}$ s	T_{Switch}= 21.2 K

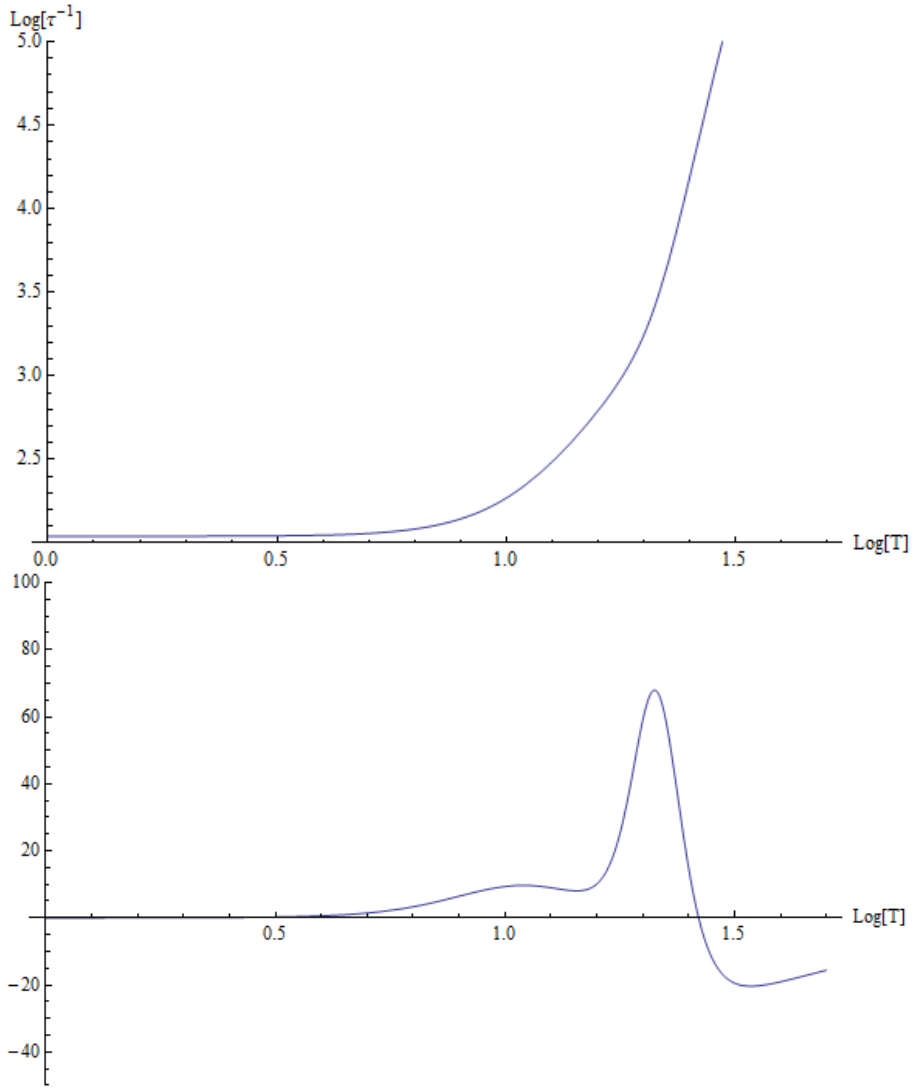

Figure S19. Relaxation rate data (**top**) for [Tb(Cp*)$_2$(BPh$_4$)] (dilute) plotted as log[τ^{-1}] vs log[T] using literature fitted parameters. The double derivative is illustrated **below** to indicate the determination of τ_{Switch}.

References

S1 S.-M. Chen, J. Xiong, Y.-Q. Zhang, Q. Yuan, B.-W. Wang and S. Gao, *Chem. Sci.*, 2018, **9**, 7540–7545.

S2 K. R. Meihaus and J. R. Long, *J. Am. Chem. Soc.*, 2013, **135**, 17952–17957.

S3 S.-D. Jiang, B.-W. Wang, H.-L. Sun, Z.-M. Wang and S. Gao, *J. Am. Chem. Soc.*, 2011, **133**, 4730–4733.

S4 L. Ungur, J. J. Le Roy, I. Korobkov, M. Murugesu and L. F. Chibotaru, *Angew. Chemie Int. Ed.*, 2014, **53**, 4413–4417.

S5 Y.-S. Meng, C.-H. Wang, Y.-Q. Zhang, X.-B. Leng, B.-W. Wang, Y.-F. Chen and S. Gao, *Inorg. Chem. Front.*, 2016, **3**, 828–835.

S6 J. J. Le Roy, I. Korobkov and M. Murugesu, *Chem. Commun.*, 2014, **50**, 1602–1604.

S7 J. J. Le Roy, L. Ungur, I. Korobkov, L. F. Chibotaru and M. Murugesu, *J. Am. Chem. Soc.*, 2014, **136**, 8003–8010.

S8 P. Zhang, L. Zhang, C. Wang, S. Xue, S. Y. Lin and J. Tang, *J. Am. Chem. Soc.*, 2014, **136**, 4484–4487.
S9 N. Ishikawa, M. Sugita, N. Tanaka, T. Ishikawa, S. Koshihara and Y. Kaizu, *Inorg. Chem.*, 2004, **43**, 5498–5500.
S10 S. Takamatsu, T. Ishikawa, S. Koshihara and N. Ishikawa, *Inorg. Chem.*, 2007, **46**, 7250–7252.
S11 C. R. Ganivet, B. Ballesteros, G. De La Torre, J. M. Clemente-Juan, E. Coronado and T. Torres, *Chem. - A Eur. J.*, 2013, **19**, 1457–1465.
S12 D. Tanaka, T. Inose, H. Tanaka, S. Lee, N. Ishikawa and T. Ogawa, *Chem. Commun.*, 2012, **48**, 7796–7798.
S13 S. Demir, J. M. Zadrozny and J. R. Long, *Chem. - A Eur. J.*, 2014, **20**, 9524–9529.